

# INFLUENCE OF RADIAL CLEARANCES ON THE AERODYNAMIC PERFORMANCE OF ORC SCROLL EXPANDERS MADE OF VARIABLE WALL THICKNESSES

Simon Emhardt<sup>1</sup>, Guohong Tian<sup>1\*</sup>, John Chew<sup>1</sup>

<sup>1</sup> Department of Mechanical Engineering Sciences, University of Surrey, Guildford, Surrey, GU2 7XH, UK

\*Corresponding author. E-mail address: [g.tian@surrey.ac.uk](mailto:g.tian@surrey.ac.uk)

## ABSTRACT

Higher efficiencies and more compact designs in spite of larger built-in volume ratios are associated with variable wall thickness scroll expander geometries. In this research paper, transient 3D CFD simulations of this scroll-type design were presented to examine the influence of radial clearances on the aerodynamic performance in small scale Organic Rankine cycle systems. The decrease of radial clearances resulted in high speed flank leakages. There was a sharp increase in the Mach number in conjunction with a decrease in the static pressure. Supersonic flows were generated through those gaps between the fixed and orbiting scroll. Thus, the radial clearances need to be sealed.

**Keywords:** Scroll expander, Variable wall thickness geometry, ORC system, Aerodynamic performance, Radial clearance, Flank leakage

## 1. INTRODUCTION

The performance of scroll expanders in small scale Organic Rankine cycle (ORC) systems is strongly influenced by its geometrical design. In particular, large built-in volume ratios are required to operate the expanders at high pressure ratios. This, in turn, facilitates the increase of the mechanical power delivered by the expander shaft [1,2]. However, the extension of the scroll profile length to increase the built-in volume ratio disadvantaged the scroll efficiency in the numerical investigation of Clemente et al. (2012) [2] due to enormous heat transfer losses. Over- and under-expansion losses were also considered by their model in addition to internal leakages through the clearances and friction between inner parts. Scroll expander geometries

made of variable wall thicknesses should reach higher efficiencies as a result of their more compact designs along with shorter scroll profile lengths and fewer number of working chambers [3-5]. Nevertheless, it is unknown whether potential higher pressure gradients in between two adjacent working chambers of these novel expander designs might cause higher losses due to high speed internal leakages.

Hence, transient and three-dimensional CFD simulations of this scroll-type design were performed in this research paper. The impact of radial clearances on the aerodynamic performance in small-scale ORC applications was examined. No lubricant oil was used to seal these clearances.

## NOMENCLATURE

<i>Abbreviations</i>	
CFD	Computational fluid dynamics
in	Inlet
NIST	National Institute of Standards and Technology
ORC	Organic Rankine cycle
PISO	Pressure Implicit with Splitting of Operators
RNG	Re-Normalization Group
URANS	Unsteady Reynolds-Averaged Navier-Stokes
<i>Symbols</i>	
Ma	Mach number (-)
n	Rotational speed (rpm)
$P_s$	Static pressure (MPa)
$P_t$	Total pressure (MPa)
$T_t$	Total temperature (K)
$\Delta t$	Physical time step (s)

## 2. GEOMETRICAL MODEL

The involute of a circle was combined with high order curves and a non-working arc to create the three-dimensional geometrical model of the variable wall thickness scroll expander as illustrated in Fig. 1. The dual arc tip design was used to form the scroll tips. All the necessary equations can be found in the work of Bin et al. (2016) [6,7].

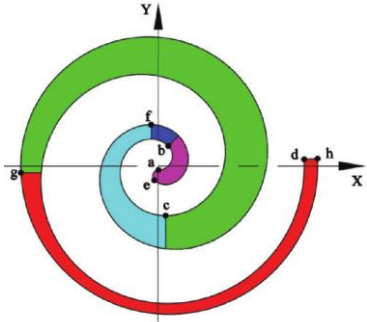


Fig. 1: Scroll geometrical model [6,7]

## 3. NUMERICAL APPROACH

The following section describes the generation of the computational grid and the numerical methods which were applied to run a transient and three-dimensional CFD simulation for a variable wall thickness scroll expander. The numerical approach of the current CFD model was already presented in the authors' previous work [8].

### 3.1 Grid generation

The computational grid was created based on a three-dimensional and unstructured grid approach as depicted in Fig. 2. The deforming working chambers along with the circular motion of the orbiting scroll were generated by means of the dynamic mesh technology of ANSYS Fluent 18.0. Two different grids for scroll expanders using radial clearances of  $200\mu\text{m}$  and  $75\mu\text{m}$  were produced. The axial clearances were neglected in both cases. The number of cells and nodes of each grid are listed in Table 1.

### 3.2 CFD model assumptions

The unsteady URANS (Unsteady Reynolds-Averaged Navier-Stokes) approach in combination with the RNG- $k-\epsilon$  turbulence model, derived from the renormalization

group theory, was utilised to carry out the CFD simulations. The Navier-Stokes equations were solved using the PISO-algorithm (Pressure Implicit with Splitting of Operators). The physical time step was specified as  $\Delta t=5e-5s$ . The pressure ratio of 4.5 was defined by imposing a total pressure of 1.485MPa and a static pressure of 0.33MPa at the scroll expander inlet and outlet in each case. The total temperature at the inlet was set to 425K and the rotational speed was fixed at  $n=2000\text{rpm}$ . The working fluid properties of the refrigerant R123 were modelled with the help of the REFPROP database from the NIST (National Institute of Standards and Technology) real gas model library.

Table 1: Mesh report

Grid	Number of nodes	Number of cells
$200\mu\text{m}$	496k	685k
$75\mu\text{m}$	641k	891k

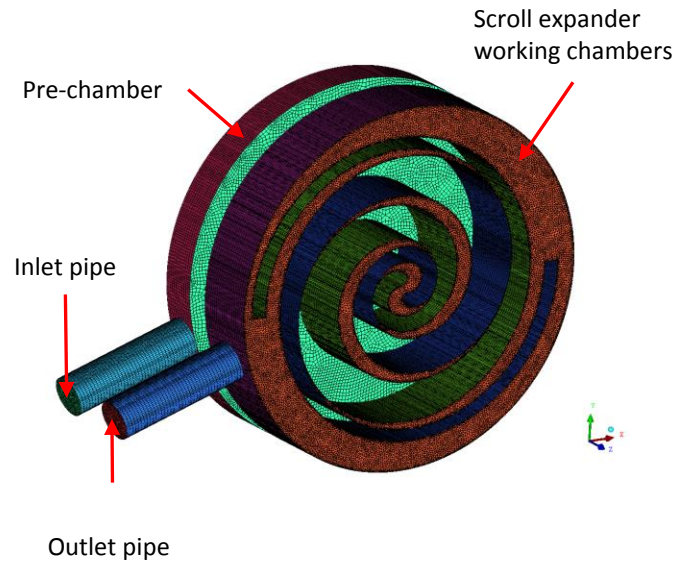


Fig. 2: Computational grid

## 4. RESULTS & DISCUSSION

The following section describes the influence of radial clearances on the aerodynamic performance of variable wall thickness scroll expanders. The flow through the radial clearance between suction and expansion chamber 2 (E2) was examined as illustrated in Fig. 3 and compared for two different radial clearances of  $200\mu\text{m}$  and  $75\mu\text{m}$  respectively. The suction port was fully closed. Fig. 3 depicts the Mach number distribution in a vertical plane parallel to the xy-layer and at a scroll height of 10mm for the radial clearance of  $75\mu\text{m}$ . It was found that

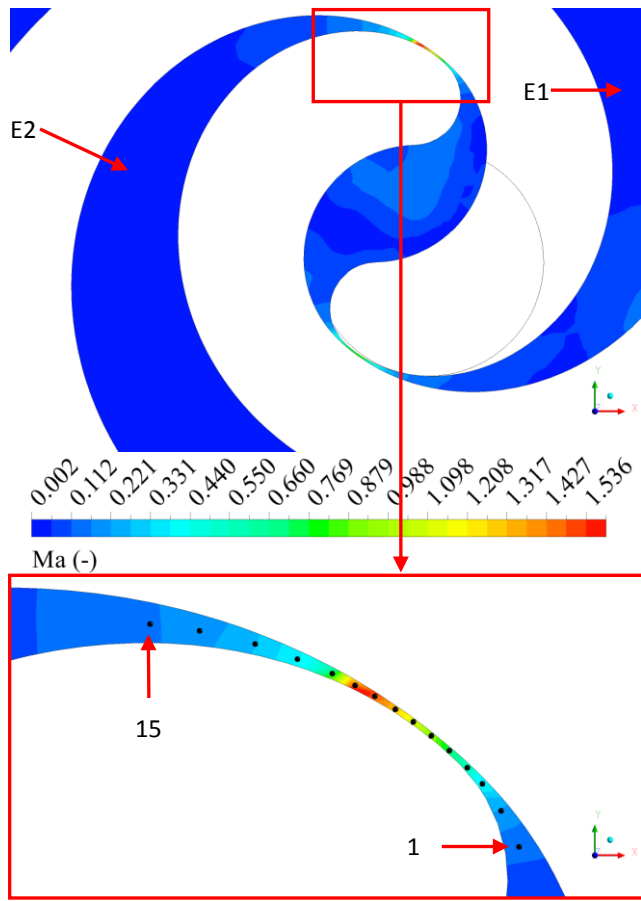


Fig. 3: Mach number distribution in a vertical plane parallel to the xy-layer ( $z=10\text{mm}$ ) for the radial clearance of  $75\mu\text{m}$

the blocking effect of the suction port caused an imbalanced pressure field in expansion chambers E1 and E2 with lower pressure values in expansion chamber E2. This, in turn, resulted in a Mach number increase up to 1.536 compared to approximately 1 through the radial clearances between suction and expansion chamber E2 as shown in Fig. 3. Besides, it can be noted that the Mach number increased along with the narrowing gap between the fixed and orbiting scroll until it reached a value of 1 in its narrowest cross section. The Mach number further increased immediately thereafter until it reached its peak value of 1.536 before it dropped as soon as the radial clearance enlarged. The radial clearance between the fixed and orbiting scroll has a similar structure as a convergent-divergent Laval nozzle. Fig. 4 illustrates the impact of the radial clearance ( $200\mu\text{m}$  vs.  $75\mu\text{m}$ ) on the static ( $P_s$ ) and total ( $P_t$ ) pressure-, total ( $T_t$ ) temperature- and Mach number ( $Ma$ ) distributions in non-dimensional form respectively. The fifteen black points plotted in Fig. 3 were utilised to evaluate the aforementioned quantities through the radial clearance

between suction and expansion chamber E2. The non-dimensional total temperature did not change along with the radial clearance in both cases and was therefore equal to 1 due to the assumption of an adiabatic system. It can be seen that the non-dimensional total pressures remained constant along the narrowing part of the clearance. The total pressures dropped as soon as the flow passed through the narrowest cross section between suction and expansion chamber E2. The total pressures remained constant at a lower level as soon as the gap between the fixed and orbiting scroll slightly widened and the flow entered expansion chamber E2 which resulted in the expansion of the working fluid. Besides this, the drop for the radial clearance of  $75\mu\text{m}$  occurred earlier in contrast to that for the radial clearance of  $200\mu\text{m}$ . The smaller cross section of the radial clearance of  $75\mu\text{m}$  also caused flank leakages with higher speeds and higher pressure drops. The non-dimensional total pressures plateaued at 0.72 ( $200\mu\text{m}$ ) compared to 0.64 ( $75\mu\text{m}$ ) as soon as the flows entered the widening part of the clearance. The non-dimensional static pressures were equal to 0.587 and 0.560 for the radial clearances of  $75\mu\text{m}$  and  $200\mu\text{m}$  as soon as the critical conditions in the throat ( $Ma=1$ ) were reached and the flows were choked. Furthermore, a large static pressure drop from 0.989 to 0.252 and from 0.909 to 0.320 can be seen respectively. The reason for a higher pressure drop for the lower radial clearance lied in its smaller cross section associated with flank leakages which had a higher speed. An abrupt and sharp static pressure increase between point 10 and 12 ( $75\mu\text{m}$ ) and 11 and 13 ( $200\mu\text{m}$ ) can be seen which reached a plateau as a result of the widening gap between the fixed and orbiting scroll. It can be determined from Fig. 4 that the Mach number for the radial clearance of  $75\mu\text{m}$  increased from 0.130 in point 1 up to 1 through the throat until it reached its peak of 1.492 in point 9 before it finally dropped back to 0.169. In contrast to the radial clearance of  $200\mu\text{m}$  through which the Mach number raised from 0.315 to 1.432 and finally dropped to 0.326. In other words, the flows were subsonic until the narrowest cross section was reached before they became supersonic immediately afterwards. The flows became subsonic again which can be seen as a sharp deceleration of the Mach number back to their original level before the flows entered the radial clearance. The acceleration and deceleration of the flows through the radial clearance occurred following the pressure changes. High built-in volume ratios are associated with the application of high pressure ratios leading to higher loss of pressure during

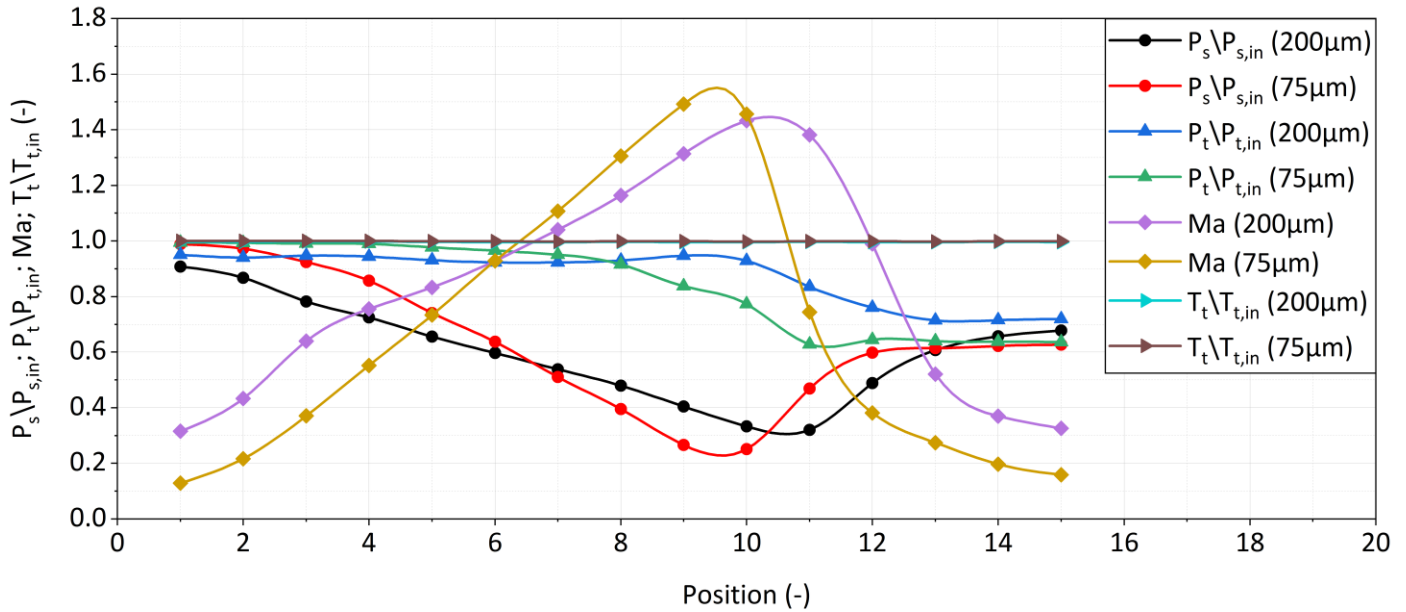


Fig. 4: Impact of decreasing radial clearances (200µm to 75µm) on the scroll expander aerodynamic performance

the expander working process which in turn contributed to those Mach number effects. More details about all the phenomena which took place here will be discussed in our future publications. In summary, it can be said that the comparison of the two cases (200µm vs. 75µm) led to the conclusion that the decrease of the radial clearances produced high speed flank leakages through those gaps. The radial clearances need to be sealed by including a refrigerant oil.

## 5. CONCLUSIONS

Three-dimensional and unsteady CFD investigations were conducted to examine the influence of radial clearances on the aerodynamic performance of small scale ORC scroll expanders using variable wall thicknesses. The pressure ratio of 4.5 was applied at two scroll expanders with radial clearances of 200µm to 75µm respectively. The rotational speed was specified to 2000rpm. The decrease of radial clearances resulted in high speed flank leakages. There was a sharp increase in the Mach number in conjunction with a sharp decrease in the static pressure through the radial clearances. Supersonic flows were generated through those gaps between the fixed and orbiting scroll. Hence, the radial clearances need to be sealed.

## REFERENCES

- [1] S. Emhardt, G. Tian, and J. Chew. A review of scroll expander geometries and their performance. *Applied Thermal Engineering* 141, pages 1020-1034, 2018
- [2] J.-C. Chang, C.-W. Chang, T.-C. Hung, J.-R. Lin, and K.-C. Huang. Experimental study and CFD approach for scroll type expander used in low-temperature organic Rankine cycle. *Applied Thermal Engineering* 73, pages 1444-1452, 2014
- [3] J.W. Bush and W.P. Beagle. Derivation of a general relation governing the conjugacy of scroll profiles. in: *Proc. International Compressor Engineering Conference, Purdue, Paper 902, 1992*
- [4] J.W. Bush, W.P. Beagle, and M.E. Housman. Maximizing scroll compressor displacement using generalized wrap geometry, in: *Proc. Int. Compress. Eng. Conf., Purdue, Paper 981, 1994*
- [5] J. Gravesen, C. Henriksen. The geometry of the scroll compressor, *Siam Rev.* Vol. 43, No. 1, pages 113–126, 2001
- [6] P. Bin, V. Lemort, A. Legros, Z. Hongsheng, and G. Haifeng. Variable thickness scroll compressor performance analysis – part I: Geometric and thermodynamic modelling. in: *Proc. IMechE. Part E: Journal of Process Mechanical Engineering* Vol. 231, pages 633-640, 2016
- [7] P. Bin, V. Lemort, A. Legros, Z. Hongsheng, and G. Haifeng. Variable thickness scroll compressor performance analysis – part II: Dynamic modelling and model validation. in: *Proc. IMechE. Part E: Journal of Process Mechanical Engineering* Vol. 231, pages 641-649, 2016
- [8] S. Emhardt, P. Song, G. Tian, J. Chew, and M. Wei. CFD analysis of variable wall thickness scroll expander integrated into small scale ORC systems. *Energy Procedia* 158, pages 2272-2277, 2019